PHYSICAL REVIEW B VOLUME 23, NUMBER 8 15 APRIL 1981

Model Hamiltonian of donors in indirect-gap materials

Yia-Chung Chang, T. C. McGill, and D. L. Smith
California Institute of Technology, Pasadena, California 91125
(Received 16 July 1980)

We propose a model Hamiltonian for donors in Si and Ge, whose matrix elements can be expressed analytically for Slater-type basis wave functions defined in an ellipsoidal coordinate system. This model Hamiltonian yields results for the energy eigenvalues of the ground state and excited states almost identical to that for the exact Hamiltonian. The simplicity of this model Hamiltonian makes the application to more complicated systems such as donor bound excitons and bound multiexciton complexes possible.

I. INTRODUCTION

The bound excited states for the donors in indirect materials, such as Si and Ge, have been successfully described by the Kohn-Luttinger effective-mass approximation (EMA).[1-3] The ground states, however, because of the multivalley nature of the conduction band, are split into several states through the "valley-orbit interaction." As a result, the binding energy is increased substantially (about 35%) and a theory beyond the EMA is required. Moreover, the effect of valley-orbit splitting is extended to several s-like excited states because they have the same symmetries as the ground states, and their wave functions have to be modified to become orthogonalized to the new ground-state wave functions. The splittings of the $2s$ states for donors in Si were estimated to be about 1 meV by Kohn and Luttinger,[2] using the quantum-defect method. This, again, cannot be explained by the EMA.

To account for the valley-orbit splittings, Baldereschi[4] performed a quantitative calculation based on the multivalley effective-mass equation (MV-EME) originally introduced by Fritzsche.[5] Later, the MV-EME was also adopted by several authors[6-10] to calculate the ground-state energies of donors in Si and Ge. Although the above calculations have produced results for Si in good agreement with experiment, it has been pointed out[11,12] that the MV-EME they used is inappropriate, because it includes spurious intervalley kinetic energy (KE) terms and neglects the overlap effects from Bloch functions in different valleys. By totally ignoring the intervalley KE terms and retaining the Bloch functions, Shindo and Nara[11] proposed another multivalley effective-mass equation. Recently, Altarelli *et al.*[13] used this new MV-EME, introducing an umklapp renormalization factor for the impurity potential due to the umklapp processes, and obtained the ground-state energies for Si:P and Ge:As in good agreement with experiment. However, as pointed out by Herbert and Inkson,[14] the neglect of intervalley KE terms could lead to unstable solution to the MV-EME, i.e., the binding energy is increased by about two orders of magnitude. Therefore, besides the umklapp processes for the impurity potential, the correct theory for the valley-orbit interaction should also include the intervalley kinetic energies in a proper way. Most recently, Resca and Resta[15,16] (RR) have proposed a "spatial renormalization factor" (SRF) to replace the umklapp renormalization factor (URF) used by Altarelli *et al.*[13] With the use of SRF, they find that both the substitutional and interstitial donors in Si introduce a deep level.[16] Unfortunately, the RR approach also neglected the intervalley KE term, which is of the same size as the intravalley KE term when the envelope function becomes very localized (necessary for a deep level). As will be shown in this paper, without the intervalley KE term, the use of URF also produces a deep level (unstable solution), whereas the introduction of intervalley KE stabilizes the system for substitutional donors.

To account for the anisotropy of the conduction band of Si and Ge, elaborate trial wave functions (for instance, the linear combinations of ellipsoidal orbitals as used by Faulkner[3] for the EMA) must be used in order to produce reasonable results. The use of elaborate trial wave functions would make the evaluation of energy expectation values very complicated and further progress, such as solving the donor bound exciton problem, very difficult.

The purpose of the present paper is twofold: (i) to provide an accurate calculation of the ground states and the s-like excited states for donors in Si and Ge with the intervalley kinetic energies and mass anisotropy taken into account properly; and (ii) to propose a model Hamiltonian, such that when the ellipsoidal trial wave functions are used, the Hamiltonian matrix elements can be expressed analytically and give rise to the correct energy values for the ground states and all excited states. We obtained energy eigenvalues of the six lowest $s(d)$-like states for various donors in

Si and Ge which are in excellent agreement with the experimental data for both the exact and the model Hamiltonians.

In Sec. II, the general theory for an impurity system is reviewed, and the model Hamiltonian is formulated. In Sec. III, the matrix elements of the exact Hamiltonian are evaluated, and the analytic expressions for the matrix elements of the model Hamiltonian are given. It is also shown that with suitable choice of some parameters, the model Hamiltonian can produce matrix elements which are almost exactly the same as those of the exact Hamiltonian. In Sec. IV, the numerical results for the exact Hamiltonian and model Hamiltonian are presented and shown to be almost identical. Finally, in Sec. V, a summary is presented.

II. THEORY

A. Basic problem

The single-particle Schrödinger equation of the perfect crystal perturbed by a substitutional impurity can be written as

$$\left(\frac{-\hbar^2}{2m}\nabla^2+(V^0+V)\right)\psi=E\psi \ , \tag{1}$$

where V^0 is the self-consistent potential seen by each electron in the perfect crystal and V is the perturbation potential introduced by the impurity. Equation (1) can be rewritten for a pseudowave function $\phi(\vec{r})$

$$\left(\frac{-\hbar^2}{2m}\nabla^2+V_\phi^0+V_\phi\right)\phi(\vec{r})=E\phi(\vec{r}) \ , \tag{2}$$

where V_ϕ^0 and V_ϕ are the pseudopotentials for the perfect crystal and impurity,[9] respectively. Using the solutions to the problem without the impurity,

$$\left(\frac{-\hbar^2}{2m}\nabla^2+V_\phi^0\right)\phi_{nk}^0(\vec{r})=E_n^0(\vec{k})\phi_{nk}^0(\vec{r}) \ ,$$

we can expand the solution to Eq. (2):

$$\phi(\vec{r})=\sum_{nk}F_n(\vec{k})\phi_{nk}^0(\vec{r}) \ . \tag{3}$$

Substituting Eq. (3) into Eq. (2), one obtains[11]

$$\begin{aligned}HF_n(\vec{k})&=E_n^0(\vec{k})F_n(\vec{k})\\&\quad+\sum_{n'k'}\langle\phi_{nk}^0|V_\phi|\phi_{n'k'}^0\rangle F_{n'}(\vec{k}')\\&=EF_n(\vec{k}) \ .\end{aligned} \tag{4}$$

For shallow donors, the wave functions are localized near the conduction-band edges. If the other bands are separated by large energy gaps as compared to the binding energies, then one has to consider only one band. This is the case for Ge where the valleys are at the zone edge in the [111] direction. In Si, however, the valleys are near the zone edge in the [100] direction and the $\Delta_{2'}$ band and Δ_1 band are degenerate at the X point.[17] In this case, substantial mixing of the two bands in the wave function $\phi(\vec{r})$ is expected. The multivalley problem for donors in Si is therefore intrinsically a two-band problem as recently pointed out by Pantelides.[18] An equivalent formulation is to allow $\vec{k}$ to range over more than one Brillouin zone with a different zone for each band.[19] In this formulation

$$\begin{aligned}HF(\vec{k})&\equiv E^0(\vec{k})F(\vec{k})\\&\quad+\sum_{k'}\langle\phi_k^0|V_\phi|\phi_{k'}^0\rangle F(\vec{k}')=EF(\vec{k}) \ .\end{aligned} \tag{5}$$

The conduction band of Si can still be approximated very well by a parabolic function.[17] The extension of the wave function $F(\vec{k})$ into the second Brillouin zone automatically takes into account the mixing with the $\Delta_{2'}$ band.

For indirect zinc-blende semiconductors, the conduction band has several equivalent minima located at $\vec{k}_j$, where j ranges over the N equivalent valleys. The value of N is 6 and 4, respectively, for Si and Ge. Since the total Hamiltonian H is invariant under the point group T_d, its eigenstates should transform as the partners of certain irreducible representations, Γ, under the operations of T_d. We can write the solution to Eq. (5) with a given summetry Γ as linear combinations of the above functions $F_j(\vec{k}-\vec{k}_j)$ localized at N equivalent valleys,[2] namely,

$$F_\Gamma^\sigma(\vec{k})=\sum_{j=1}^{N}\alpha_j^\sigma(\Gamma)F_j(\vec{k}-\vec{k}_j) \ , \tag{6}$$

where the coefficients $\alpha_j^\sigma(\Gamma)$ are determined by group theory. σ labels the degenerate partners and the wave functions $F_j(\vec{k}-\vec{k}_j)$ are related to one another simply by the operations belonging to the group T_d. It is clear that if the functional form of $F_j(\vec{k}-\vec{k}_j)$ is known for a given valley, then the total wave function $F_\Gamma^\sigma(\vec{k})$ is completely determined by Eq. (6). If we expand the function $F_\Gamma^\sigma(\vec{k})$ on a complete orthonormal set of functions $\{\sum_j\alpha_j^\sigma\beta_\nu^j(\vec{k}-\vec{k}_j)\}$, then we have, for the jth valley,

$$F_j(\vec{k}-\vec{k}_j)=\sum_\nu C_\nu\beta_\nu^j(\vec{k}-\vec{k}_j) \ . \tag{7}$$

Substituting Eq. (7) in Eq. (5), we obtain after the application of symmetry[8]

$$\sum_\nu H_{\mu\nu}C_\nu=E\sum_\nu N_{\mu\nu}C_\nu \ , \tag{8}$$

where

$$H_{\mu\nu}=\sum_{\lambda=1}^{m}g_\lambda(\Gamma)H_{\mu\nu}^{(\lambda)} \ , \tag{9}$$

and

$$N_{\mu\nu}=\sum_{\lambda=1}^{m} g_\lambda(\Gamma)N_{\mu\nu}^{(\lambda)} \ . \tag{10}$$

$H_{\mu\nu}^{(\lambda)}$ and $N_{\mu\nu}^{(\lambda)}$ are the matrix elements for the basis wave functions associated with the intravalley ($\lambda=1$), intertransverse ($\lambda=2$), and interlongitudinal ($\lambda=3$) terms. All three terms are present in Si ($m=3$); the last term ($\lambda=3$) is absent in Ge ($m=2$). The coefficients $\{g_\lambda(\Gamma)\}$ which are obtainable from symmetry can be found in Refs. 8 and 10.

B. Formulation of the model Hamiltonians

In this section, we derive an expression for model Hamiltonians (one for each possible irreducible representation) which operates on the envelope function for a single valley. We obtain *closed form*, approximate expressions for these Hamiltonians. This is accomplished by neglecting intervalley overlap matrix elements which can be shown to yield very small corrections ($\lesssim 0.1\%$) to the energy eigenvalues.

Returning to Eq. (5), we can write H as the sum of the kinetic-energy operator T and the potential-energy operator V. We first examine the potential-energy part of H. V is an integral operator whose kernel is defined by $\langle\phi_k^0|V_\phi|\phi_{k'}^0\rangle$. The pseudoimpurity potential V_ϕ can be written as a point-charge potential $V_{\rm PC}(\vec{r})$ plus a short-range core potential $W(\vec{r})$.

Because of its short-range nature, the Fourier transform of $W(\vec{r})$ should be a smooth function over the appropriate region in k space. Hence we can assume that the matrix element of $W(\vec{r})$ for $\vec{k}$ and $\vec{k}'$ near the band minima are given by

$$\langle\phi_{k_i}^0|W|\phi_{k_j}\rangle\equiv J_\lambda \ , \tag{11}$$

where J_λ takes on three values depending on whether $\vec{k}_i$ and $\vec{k}_j$ are in the same valley ($\lambda=1$), on different axes ($\lambda=2$), or on the same axis ($\lambda=3$). The point-charge part can be written approximately as

$$\langle\phi_k^0|V_{\rm PC}|\phi_{k'}^0\rangle=R_\lambda\tilde{V}_{\rm PC}(\vec{k}-\vec{k}') \ , \tag{12}$$

where $\tilde{V}_{\rm PC}(\vec{q})=-4\pi e^2/q^2\epsilon(\vec{q})$ is the Fourier transform of $V_{\rm PC}(\vec{r})$ with $\epsilon(\vec{q})$ being the wave-vector-dependent dielectric function which is customarily represented by the empirical form[20–22]

$$\frac{1}{\epsilon(\vec{q})}=\frac{Aq^2}{q^2+\alpha^2}+\frac{(1-A)q^2}{q^2+\beta^2}+\frac{1}{\epsilon(0)}\frac{\gamma^2}{q^2+\gamma^2} \ , \tag{13}$$

and R_λ are the umklapp renormalization factors as defined in Ref. 13. As before, λ implies the relationship between $\vec{k}_i$ and $\vec{k}_j$, the centers of the ith and jth valleys, respectively. For any two basis functions $\beta_\mu^i(\vec{k}-\vec{k}_i)$ and $\beta_\nu^j(\vec{k}-\vec{k}_j)$, the potential matrix element is given by

$$V_{\mu\nu}^{(\lambda)}=J_\lambda\beta_\mu^{i*}(0)\beta_\nu^j(0)+R_\lambda\int d^3r e^{i(\vec{k}_j-\vec{k}_i)\cdot\vec{r}}\times V_{\rm PC}(\vec{r})\beta_\mu^{i*}(\vec{r})\beta_\nu^j(\vec{r}) \ , \tag{14}$$

where $\beta_\nu^j(\vec{r})e^{i\vec{k}_i\cdot\vec{r}}$ be the Fourier transform of $\beta_\nu^j(\vec{k}-\vec{k}_i)$ in real space, and similarly for $\beta_\nu^j(\vec{r})e^{i\vec{k}_j\cdot\vec{r}}$.

We now derive a functional form for the potential term for the model Hamiltonians, which yields analytic expressions for the basis functions defined in an ellipsoidal coordinate system. All the materials treated in this paper have very anisotropic conduction bands. If we define the ratio of the longitudinal effective mass m_l to the transverse effective mass m_t as the "anisotropy factor" μ, then the values of μ are about 5 for Si and 20 for Ge. To account for the anisotropic charge distribution caused by the kinetic-energy term, we choose the basis functions to take the form $\beta_\mu(\vec{r}')$, with the argument $\vec{r}'$ defined as

$$\vec{r}'=(x,y,z/\zeta) \ , \tag{15}$$

where the parameter ζ is called the "eccentricity factor." The appropriate eccentricity factor ζ can be determined by a variational calculation, where the energy expectation value of the lowest-lying state of certain symmetry is minimized. When ellipsoidal basis wave functions are used, it is convenient to write the point-charge potential $V_{\rm PC}(\vec{r})$ in an ellipsoidal coordinate system as well,

$$V_{\rm PC}(\vec{r})=-\frac{e^2}{\epsilon[r'(1-g^2\cos^2\theta')^{1/2}]r'(1-g^2\cos^2\theta')^{1/2}} \ , \tag{16}$$

with $g^2\equiv 1-\zeta^2$ and θ' is the polar angle in an ellipsoidal coordinate system. The matrix elements $V_{\mu\nu}^{(\lambda)}$ in Eq. (14) are rather complicated, since the term $(1-g^2\cos^2\theta')^{1/2}$ mixes states of angular momentum quantum number differing by an even integer. For s-like wave functions we choose the model potential to have the form (see Appendix A for derivation of this functional form)

$$V_{\rm SM}^{(\lambda)}(\vec{r}')=\frac{J_\lambda\delta(\vec{r}')}{\zeta}-R_\lambda\frac{e^2}{\epsilon'(r')r'}\frac{f_\lambda a_0\sin(p_\lambda\Delta r')}{(p_\lambda\Delta r')} \ , \tag{17}$$

where

$$a_0\equiv(\sin^{-1}g)/g \ , \qquad \Delta\equiv 2\zeta k_0 \ , \tag{18}$$

and

$$\frac{1}{\epsilon'(r')} \equiv \frac{1}{\epsilon_0} \sum_{\nu=1}^{4} S_\nu e^{-h\sigma_\nu r'} , \tag{19a}$$

with

$$S_\nu = [1, A\epsilon_0, (1-A)\epsilon_0, -1] \tag{19b}$$

and

$$\sigma_\nu = (0, \alpha, \beta, \gamma) . \tag{19c}$$

f_λ, p_λ, and h are adjustable parameters obtained by minimizing the differences between the matrix elements of this model potential and the exact matrix elements $V_{\mu\nu}^{(\lambda)}$. As will be shown in Sec. III, with suitable choice of the parameters f_λ, p_λ, and h the matrix elements of the model potential can fit the exact matrix elements extremely well. For non-s-like states, which are only important for the expansion of excited states and have vanishing amplitude near the origin, the short-range correction and intervalley scattering terms are negligible. Thus, the effective potential is simply the hydrogenic potential screened by the dielectric constant ϵ_0.[2] Hence, the total model potential operator can be written approximately as

$$V_M^\Gamma(\vec{r}') \simeq \sum_\lambda g_\lambda(\Gamma) V_{SM}^{(\lambda)} |0\rangle\langle 0| - \frac{e^2}{\epsilon_0 r'(1-g^2\cos^2\theta')^{1/2}}(1-|0\rangle\langle 0|) , \tag{20}$$

where $|0\rangle\langle 0|$ is the projection operator onto $l=0$ states.

The $\vec{q}$ dependence of the dielectric function, short-range core potential, and the intervalley scattering terms have been neglected for the mixing of s-like states with non-s-like states.

The next step is to examine the kinetic energy (KE) part of the total Hamiltonian. In general, the KE matrix elements $T_{\mu\nu}^{(\lambda)}$ can be calculated exactly by carrying out the integration in k space, i.e.,

$$T_{\mu\nu}^{(\lambda)} = \int \beta_\mu^i(\vec{k}-\vec{k}_i) E^0(\vec{k}) \beta_\nu^j(\vec{k}-\vec{k}_j) d^3k , \tag{21}$$

where the full knowledge of the dispersion function for the conduction band in the extended zone scheme is required. Because of the localized nature of the envelope wave functions in k space, it is a good approximation to write $E^0(\vec{k})$ as the sum of $E_i^0(\vec{k}-\vec{k}_i)$ defined for the ith valley as

$$E_i^0(\vec{k}-\vec{k}_i) = \hbar^2(k_x^2+k_y^2)/2m_t + \hbar^2(k_z-k_0)^2/2m_l , \tag{22}$$

where we have chosen $\vec{k}_i = k_0\hat{z}$, with k_0 being the distance of the band minimum from the zone center. For Ge, the band minimum is right on the L point. For Si, the value of k_0 used in this paper is $0.86(2\pi/a)$,[23] where a is the lattice constant. The functions $E_i(\vec{k}-\vec{k}_i)$ are truncated at the value of $\vec{k}$, where these functions centered at different valleys intersect with each other. This truncation is necessary for evaluating the intervalley KE so as to avoid the spurious overlapping of the function $\hbar^2(k_z-k_0)^2/2m_l$ with the wave functions centered at other valleys (e.g., $\vec{k}_i = -k_0\hat{z}$).[14]

For the intravalley term, this restriction is unnecessary, and the model KE operator in real space can be written as

$$T_M^{(1)}(\vec{r}) = -\frac{\hbar^2}{2m_l}\left[\frac{\partial}{\partial z}\right]^2 - \frac{\hbar^2}{2m_t}\left[\left[\frac{\partial}{\partial x}\right]^2 + \left[\frac{\partial}{\partial y}\right]^2\right] , \tag{23}$$

where we have chosen the z axis to be the longitudinal axis. For the intervalley terms, we only have to consider the matrix elements between s-like states (the others are negligibly small). As will be shown in Sec. III, we can find a simple closed-form operator to approximate the exact intervalley KE operator (defined in ellipsoidal coordinates, $\vec{r}'$)

$$T_M^{(\lambda)}(\vec{r}') = \frac{\hbar^2}{2m_t} B\left[\left(\frac{\overleftarrow{\partial}}{\partial r'}\right)[Ce^{-\eta_\lambda \Delta r'} - (C-1)e^{-2\eta_\lambda \Delta r'}]\left(\frac{\overrightarrow{\partial}}{\partial r'}\right)\right] , \quad \lambda = 2, 3 , \tag{24}$$

with

$$B \equiv \frac{1}{3}\left[2 + \frac{1}{\mu\zeta^2}\right] , \tag{25a}$$

where $\mu \equiv m_l/m_t$ and

$$\Delta \equiv 2\zeta k_0 . \tag{25b}$$

The operators $(\partial/\partial r')$ with arrows pointing left or right, are defined as

$$\left(\frac{\overrightarrow{\partial}}{\partial r'}\right) R(r') \equiv \frac{\partial R(r')}{\partial r'} \equiv R(r')\left(\frac{\overleftarrow{\partial}}{\partial r'}\right) . \tag{26}$$

C and η_λ are chosen to minimize the differences between the model matrix elements $\langle\beta_\mu|T_M^{(\lambda)}|\beta_\nu\rangle$ and the exact ones $\langle\beta_\mu|T^{(\lambda)}|\beta_\nu\rangle$. The total model KE operator is therefore written as

$$T_M^\Gamma = T_M^{(1)} + \sum_{\lambda=2}^{3} g_\lambda(\Gamma) T_M^{(\lambda)} |0\rangle\langle 0| . \tag{27}$$

Combining Eq. (27) with Eq. (20), we therefore get the closed-form expression for the model Hamiltonian of symmetry Γ

$$H_M^\Gamma = T_M^\Gamma + V_M^\Gamma . \tag{28}$$

In the next section we derive the explicit expressions for the matrix elements of the exact Hamiltonian H and the model Hamiltonians, H_M^{Γ}, and see how closely they are related to each other.

III. MATRIX ELEMENTS

In this section, we evaluate the matrix elements for both the exact and model Hamiltonians and determine the parameters in the model Hamiltonians which give the best fit between the two sets of matrix elements. Slater orbitals in an ellipsoidal coordinate system are used as the basis set. The z axis can be used as the longitudinal axis of the ellipsoidal coordinate system. Analytic expressions for the matrix elements for the model Hamiltonians are also given. For convenience we use atomic units (a.u.) with energy measured in units of $e^4 m_t/2\epsilon_0^2\hbar^2$ (rydberg, Ry) and distance measured in units of $\epsilon_0\hbar^2/m_t e^2$ (bohr), where m_t is the transverse effective mass.

The radial part of each basis function is made up of a linear combination of ellipsoidal Slater orbitals,

$$\bar{R}_{nl}(r') = \frac{r'^{l} e^{-b_{nl} r'}}{(N_{nl})^{1/2}} , \tag{29}$$

where N_{nl} is the normalization constant,

$$N_{nl} = \frac{(2b_{nl})^{l+3/2}}{\sqrt{2l+2)!}} . \tag{30}$$

The exponents b_{nl} are chosen to cover the entire physically reasonable range. The actual basis function $\beta_{nlm}(\vec{r}')$ is formed by taking the product of a spherical harmonic $Y_{lm}(\Omega')$ with an appropriate radial function obtained from $R_{nl}(r')$ by employing the Schmidt orthogonalization procedure[24]

$$\beta_{nlm}(\vec{r}') = R_{nl}(r') Y_{lm}(\Omega') , \tag{31}$$

with

$$R_{nl}(r') = \sum_{n'} A^{l}_{nn'} \bar{R}_{n'l}(r') \tag{32}$$

with $A^{l}_{nn'}$ obtained from the Schmidt orthogonalization procedure.

A. Exact Hamiltonian

The matrix elements of the exact Hamiltonian in this basis can be written in terms of the Slater orbitals [Eq. (29)]

$$\langle \beta_{n_1' l_1 m_1} | H^{(\lambda)} | \beta_{n_2' l_2 m_2} \rangle = \sum_{n_1' n_2'} A_{n_1 n_1'} A_{n_2 n_2'} \langle \bar{R}_{n_1' l_1} Y_{l_1 m_1} | H^{(\lambda)} | \bar{R}_{n_2' l_2} Y_{l_2 m_2} \rangle . \tag{33}$$

We first calculate the matrix elements for the Hamiltonian $H^{(\lambda)}$ for two s-like Slater orbitals denoted as $|b_1\rangle$ and $|b_2\rangle$, [see Eq. (29)] where b is the exponent. The total matrix element may be divided into two parts, the kinetic energy $T^{(\lambda)}$ and the potential energy $V^{(\lambda)}$. For the intravalley term, we obtain

$$\langle b_1 | T^{(1)} | b_2 \rangle = 8B(b_1 b_2)^{5/2}/(b_1+b_2)^3 , \tag{34}$$

with B given by Eq. (25a). The intervalley kinetic-energy matrix elements can be written in terms of the Fourier transforms of Slater orbitals

$$\bar{R}_b(\vec{k}) = \frac{16\pi b^{5/2}}{(b^2 + k_x^2 + k_y^2 + \zeta^2 k_z^2)^2} . \tag{35}$$

For the intervalley ($\lambda = 2, 3$), we have

$$\langle b_2 | T^{(\lambda)} | b_1 \rangle = \frac{\zeta}{4\pi} \int \frac{d^3k}{(2\pi)^3} \bar{R}_{b_2}[0^{(\lambda)}(\vec{k} - k_0\hat{z})] E_1^0(\vec{k} - k_0\hat{z}) \bar{R}_{b_1}(\vec{k} - k_0\hat{z}) + \cdots , \tag{36}$$

where the ellipsis represents exchange term, $E_1^0(\vec{k} - k_0\hat{z})$ is defined in Eq. (22) for the valley associated with $\bar{R}_{b_1}$, $\hat{z}$ is the unit vector in the z direction, and $0^{(\lambda)}$ is a rotation operator[25] which transforms from a given valley to a transverse valley ($\lambda = 2$) or a longitudinal valley ($\lambda = 3$). The exchange term is produced by interchanging b_1 and b_2. With some approximation, Eq. (36) can be reduced to two-dimensional and one-dimensional integrals for $\lambda = 2$ and 3, respectively. For the reader's interest, we put this derivation in Appendix B.

The matrix elements of the potential energy for s-like basis states are given by

$$\langle b_1 | V^{(\lambda)} | b_2 \rangle = \frac{(b_1 b_2)^{3/2}}{\pi\zeta} \left[J_\lambda + 8\pi \sum_{\nu=1}^{4} S_\nu J_\nu^{(\lambda)}(b_1, b_2) \right] , \tag{37}$$

where S_ν is given by Eq. (19b). The functions $J_\nu^{(\lambda)}$ are given by

$$J_\nu^{(1)}(b_1,b_2)=\int_0^1 d\xi \frac{1}{\{(b_1+b_2)[1+(\delta-1)\xi^2]^{1/2}+\sigma_\nu\}^2} , \tag{38a}$$

$$J_\nu^{(3)}(b_1,b_2)=\mathrm{Re}\int_0^1 d\xi \frac{1}{(\{(b_1+b_2)[1+(\delta-1)\xi^2]^{1/2}+\sigma_\nu\}+2ik_0)^2} , \tag{38b}$$

and

$$J_\nu^{(2)}(b_1,b_2)=\mathrm{Re}\int_0^{2\pi}\frac{d\phi}{(2\pi)}\int_0^1 d\xi \frac{1}{[(b_1\nu_1+b_2\nu_2+\sigma_\nu)+ik_0(\eta_1-\eta_2)]^2} , \tag{38c}$$

where σ_ν are given by Eq. (19c),

$$\nu_{1,2}\equiv[1+(\delta-1)\eta_{1,2}^2]^{1/2} , \quad \delta\equiv\zeta^{-2} , \tag{39a}$$

and

$$\eta_{1,2}\equiv(1-\xi^2)^{1/2}\cos(\phi\pm\beta/2) , \tag{39b}$$

with $\beta=90°$ for Si and 109.47° for Ge.

As discussed in Sec. II B, the exact Hamiltonian can be approximated by the single-valley effective-mass Hamiltonian H_{EMA} for all the other basis states. These matrix elements for ellipsoidal Slater orbitals are given by[3]

$$\langle b_1 lm|H_{\mathrm{EMA}}|b_2 l'm'\rangle=\delta_{mm'}\left\{\delta_{ll'}C_l^m I_l(b_1,b_2)+D_l^m[\delta_{l,l'+2}J_{ll'}(b_1,b_2)+\delta_{l,l'-2}J_{l'l}(b_2,b_1)]\right.$$
$$\left.-\delta_{l,l'+2j}\sum_{\nu=0}^{(l+l')/2}G_{ll'}^\nu(m)a_\nu K_{ll'}(b_1,b_2)\right\} , \tag{40}$$

where j is an integer such that $l'+2j$ is non-negative. The coefficients C_l^m and D_l^m are given by

$$C_l^m\equiv 1-(1-B)\left[1+\frac{2l(l+1)-6m^2}{(2l-1)(2l+3)}\right] , \tag{41a}$$

and

$$D_l^m\equiv\frac{3(1-B)}{(2l-1)}\left[\frac{(l^2-m^2)[(l-1)^2-m^2]}{(2l+1)(2l-3)}\right]^{1/2} , \tag{41b}$$

where B is given by Eq. (25a). The coefficients a_ν are given by the recursion relation

$$a_\nu=\frac{[(2\nu-1)a_{\nu-1}-\zeta]}{2\nu g^2} \quad \text{for } \nu\geq 1 , \tag{42a}$$

with

$$a_0=\frac{\sin^{-1}g}{g} . \tag{42b}$$

The $G_{ll'}^\nu(m)$ are defined by

$$4\pi Y_{lm}^*(\Omega)Y_{l'm}(\Omega)=\sum_{\nu=0}^{(l+l')/2}G_{ll'}^\nu(m)\cos^{2\nu}\theta \tag{43}$$

and can be obtained by carrying out this expansion.[26]

The coefficients I, J, and K are given by

$$I_l(b_1,b_2)=S_{12}(l)\left[b_1b_2+b^2\frac{l}{(l+1)}\right] , \tag{44a}$$

$$J_{ll'}(b_1,b_2)=S_{12}(l)[b_2^2+2bb_2/(l+l'+2)] , \tag{44b}$$

$$K_{ll'}(b_1,b_2)=4S_{12}(l)b/(l+l'+2) , \tag{44c}$$

where

$$S_{12}(l)\equiv\langle b_1 l|b_2 l\rangle=\left[\frac{\sqrt{b_1b_2}}{b}\right]^{2l+3} \tag{45a}$$

and

$$b\equiv(b_1+b_2)/2 . \tag{45b}$$

B. Model Hamiltonian

The only part of the model Hamiltonian matrix that differs from the exact Hamiltonian matrix is that for the s-like basis states. Again we will treat the kinetic and potential energies separately.

We want to replace the intervalley contribution to the kinetic energy by that appearing to originate from a single valley.

The form of the model KE operators given in Eq. (24) is obtained by observing that the principal contribution to the integral in Eq. (36) occurs for $\bar{R}_b$ near the band minima. Hence, we can approximate

TABLE I. Adjustable parameters h, f_λ, p_λ, C, and η_λ determined by fitting the diagonal matrix elements of various terms in the model Hamiltonian with that of the corresponding terms in the exact Hamiltonian.

Parameter \ Material	Si			Ge	
	Intra ($\lambda=1$)	Inter-trans ($\lambda=2$)	Inter-long ($\lambda=3$)	Intra ($\lambda=1$)	Inter-trans ($\lambda=2$)
f_λ	1	1	2	1	1
p_λ	1	1.005	2.265	1	1.48
η_λ		1.48	1.59		2.42
h		0.821			0.69
C		12			25

the integral by replacing the tail of the basis function $\bar{R}_b$ in the other valleys by an appropriate function in the original valley.

In the first term of Eq. (36), $\bar{R}_{b_2}$ is localized in the valley outside the region where the integration is carried out. Its tail in the region of integration is a smooth function of $\vec{k}$, and can be approximated by the functional form

$$\frac{16\pi b_2^{5/2}C}{[(\eta_\lambda\Delta+b_2)^2+\zeta^2(\vec{k}-k_0\hat{z})^2]^2}-\frac{16\pi b_2^{5/2}(C-1)}{[(2\eta_\lambda\Delta+b_2)^2+\zeta^2(\vec{k}-k_0\hat{z})^2]^2}\ , \tag{46}$$

where η_λ and C are taken as adjustable parameters. This function has the advantage that it resembles the function $\bar{R}_{b_2}$ in the region of integration and only gives small contribution to the integral when the region of integration is extended to the whole k space. Furthermore, when the region of integration is extended to the whole k space, the integral can be done analytically and we obtain

$$\langle b_2|T_M^{(\lambda)}|b_1\rangle=8B(b_1b_2)^{5/2}\left[\frac{C}{(\eta_\lambda\Delta+b_1+b_2)^3}-\frac{(C-1)}{(2\eta_\lambda\Delta+b_1+b_2)^3}\right]\ , \tag{47}$$

which corresponds to the matrix elements of the postulated intervalley KE operators defined in Eq. (24). It should be noted that Eq. (47) reduces to Eq. (34) when Δ is set equal to zero.

The matrix elements for the s-like part of the model potentials $V_{SM}^{(\lambda)}$ [given in Eq. (17)] can be carried out analytically. We obtain

$$\langle b_1|V_{SM}^{(\lambda)}|b_2\rangle=8(b_1b_2)^{3/2}\left[\frac{J_\lambda}{(8\pi\zeta)}+R_\lambda\sum_{\nu=1}^{4}\frac{S_\nu a_0}{(b_1+b_2+h\sigma_\nu)^2+p_\lambda^2\Delta^2}\right]\ , \tag{48}$$

where R_λ, S_ν, and σ_ν are defined by Eqs. (12), (19b), and (19c), respectively; p_λ and h are adjustable parameters.

C. Fitting of the free parameters

There are a number of free parameters in the model Hamiltonians which are to be selected so that the matrix elements of the model Hamiltonian are as close as possible to those for the exact Hamiltonian. Fitting of this expression for the KE matrix elements results in the parameters given in Table I for Si and Ge. The quality of the fit as a function of the orbital exponent for the Slater orbital is shown in Fig. 1. The fit is superb for the range $b<8$ a.u.; however, for larger values of b (more localized functions) deviations between the exact and model results do occur.

The fit of the intravalley PE matrix elements is accomplished by adjusting the parameter h. The values

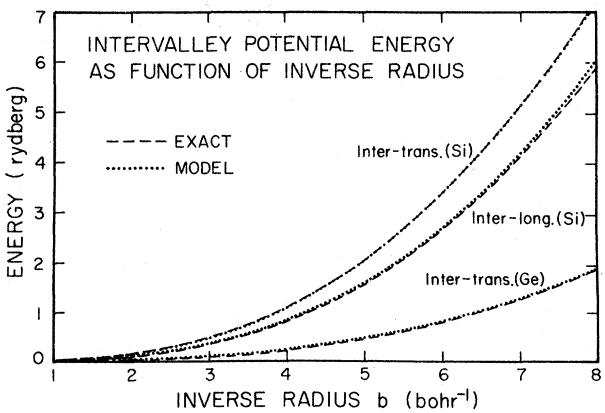

FIG. 1. Intervalley kinetic energy plotted as a function of the inverse radius of the basis envelope wave function for the exact Hamiltonian (dashed line) and the model Hamiltonian (dotted line) for donors in Si and Ge. Atomic units are used as defined in the text.

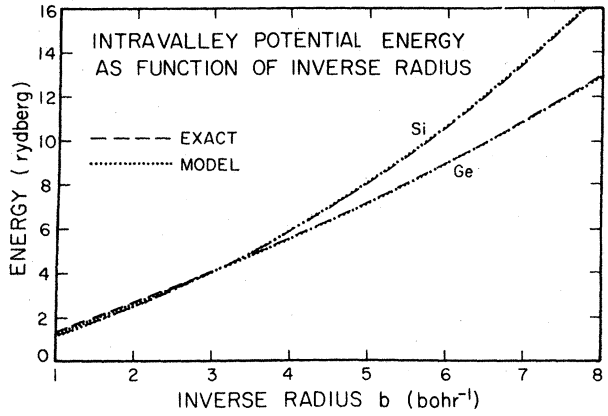

FIG. 2. Intravalley potential energy plotted as a function of the inverse radius of the basis envelope wave function for the exact Hamiltonian (dashed line) and the model Hamiltonian (dotted line) for donors in Si and Ge. Atomic units are used as defined in the text.

resulting in the best fit are given in Table I. The quality of the fit as a function of orbital exponent for the Slater orbital is shown in Fig. 2. Again the fit is superb, and continues to be quite good even for large values of b.

The fit of the intervalley PE matrix elements is carried out by adjusting the parameters p_λ and f_λ with h fixed at the value required for the intravalley PE. The parameters resulting in a very good fit are given in Table I. The comparison between the exact results and calculations for the model are given in Fig. 3. The fit is quite good over the entire range of b required for our calculations.

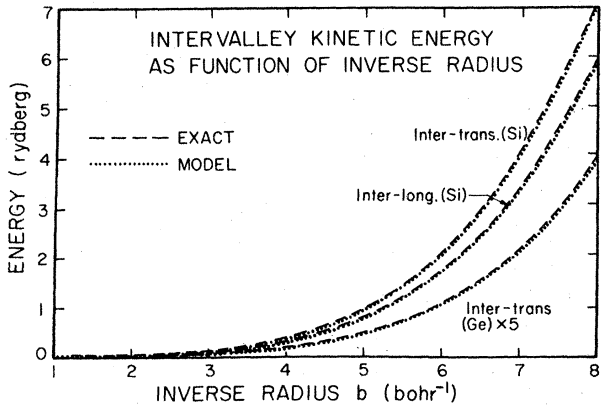

FIG. 3. Intervalley potential energy plotted as a function of the inverse radius of the basis envelope wave function for the exact Hamiltonian (dashed line) and the model Hamiltonian (dotted line) for donors in Si and Ge. Atomic units are used as defined in the text.

IV. RESULTS

In this section we report the results of calculations of the various ground states and $s(d)$-like excited states of donors in Si and Ge. Results are reported for both the model and exact Hamiltonian matrices.

The numerical work was carried out, using 10 s-like, 6 d_0-like, and 4 g_0-like Slater orbitals. The parameters b_{nl} are chosen to be b_0/Z_{nl}, with $b_0=2$ a.u. for Si and $b_0=4$ a.u. for Ge and

$$Z_{nl}=(1,1.5,2,3,4,6,9,14,0.5,0.25) \text{ for } l=0 ,$$

$$Z_{nl}=(0.5,0.7,1,2,3,5) \text{ for } l=2 ,$$

$$Z_{nl}=(0.5,0.7,1,2) \text{ for } l=4 .$$

The eccentricity factor ζ was determined by minimizing the ground-state energy. Hence, it is not clear whether our basis set is good for the excited states or not. To examine this, we calculated the eigenvalues of the EMA[2] Hamiltonian using this basis set with $\zeta=0.57$ for Si and $\zeta=0.355$ for Ge, respectively. Our results for the lowest six states are listed in Table II along with the results obtained by Faulkner.[3]

Our results for Si are almost identical to that of Faulkner.[3] For Ge, we obtain slightly larger ionization energies (by about 0.1 meV) for the excited states than those obtained by Faulkner. We therefore believe that our method is suitable for the ground states as well as for the excited states.

The matrix elements for the exact Hamiltonian H and the model Hamiltonian H_M were obtained as described in Sec. III, and both matrices are diagonalized numerically. The results obtained for both Hamiltonians are very close to each other (within 1%).

For the isocoric impurity P in Si, we assume the short-range core potential takes the form

$$W(\vec{r})=P_c e^{-\sigma_c r}\frac{27.2}{\epsilon(r)} , \tag{49}$$

in units of eV with $P_c\simeq 2.72$ and $\sigma_c\simeq 3.33$ a.u.[27] Putting Eq. (49) into Eq. (11), we obtain[28,29] that $J_1\simeq -0.60$, $J_2\simeq 6.35$, and $J_3\simeq 7.11$ (in units of 10^{-3} Ry bohr^3). For As in Ge, we assume the short-range core potential has negligible effect, i.e., set $J_\lambda=0$ in Eqs. (14), (17), and (37). The validity of this assumption may depend on the impurity pseudopotential used. It was shown by Pantelides and Sah[9] that the short-range core potential is small for an isocoric impurity, if one works within a true-potential representation. On the other hand, the umklapp renormalization factors R_λ are obtained by using the empirical pseudopotential method (EPM). This empirical pseudopotential used for the crystal may not satisfy the criteria for internal consistency given by Pantelides.[18] We therefore calculated the ground-state energies for several choices of the renormaliza-

TABLE II. Ionization energies of the six lowest $s(d)$-like states obtained in EMA for Si:P and Ge:As. The results obtained by Faulkner (Ref. 3) are also included for comparison. All energy values are in meV.

		$1s$	$2s$	$3s$	$3d_0$	$4s$	$4d_0$
Si:P	Present work	31.22	8.85	4.76	3.75	2.86	2.11
	Ref. 3	31.27	8.83	4.75	3.75	2.85	2.11
Ge:As	Present work	9.81	3.59	2.14	1.43	1.19	0.94
	Ref. 3	9.81	3.52	2.01	1.34	1.17	0.87

tion factors R_λ. For Si, we worked out the cases with R_2 taken to be from 0.47 to 0.55 and R_3 taken to be 0.48. The results for the energies of the three split ground states calculated for both H and H_M are plotted in the upper half of Fig. 4 against the parameter R_2. We find that with the choice $R_2 \simeq 0.53$, the theoretical results are in excellent agreement with the experimental data. For $R_2 = 0.38$ and $R_3 = 0.3$ (the values obtained from EPM),[13] we obtain for the Γ_1, Γ_5, and Γ_3 states 38.9, 35.1, and 33.5 meV, respectively, when $W(\vec{r})$ is included and 43.2, 34.3, and 33.1 meV, respectively, when $W(\vec{r})$ is neglected. For Ge:As, the energies of the split ground states are plotted in the lower half of Fig. 4 against R_2, with R_2 ranging from 1.3 to 1.8. For $R_2 \simeq 1.56$, the results fit experimental data very well. For $R_2 = 2.33$ (the value obtained from EPM),[13] we obtain very large binding energy (> 20 meV), which is inconsistent with the experimental data.

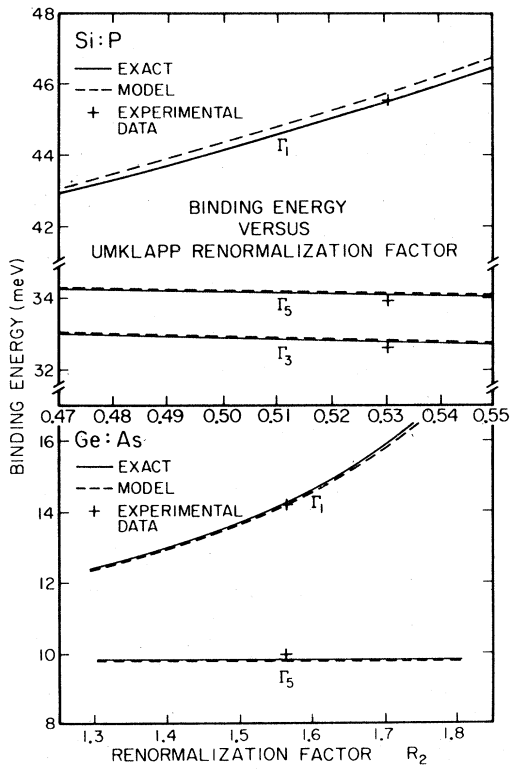

FIG. 4. Binding energies of the ground states associated with various irreducible representations plotted against the umklapp renormalization factor R_2 for the exact Hamiltonian (solid line) and the model Hamiltonian (dashed line), for Si:P (upper half) and Ge:As (lower half), respectively. The experimental data (taken from Ref. 30 for Si:P and Ref. 34 for Ge:As) are also included (marked "+"). The energy units are meV.

To examine the stability of the Hamiltonian when the short-range core potential is neglected, we did a variational calculation using the s-like trial wave function $\bar{R}_b(\vec{r})$ as given by Eq. (29). In Fig. 5 the energy expectation value of the Γ_1-symmetry ground state for Si:P with a trial wave function given by Eqs. (6) and (29) is plotted against the variational parameter b. The umklapp renormalization factors used are those from EPM.[13] As shown in this figure, the system is stabilized only if the intervalley KE term is included. Similar situations also hold for donors in Ge.

The charge densities of the ground states of Si:P

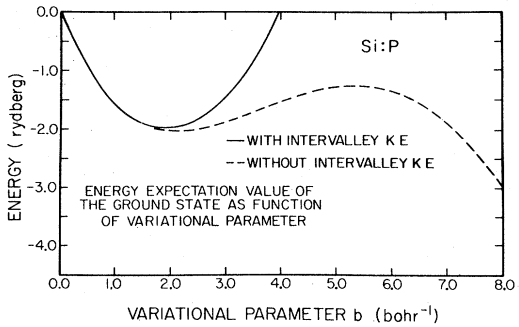

FIG. 5. Energy expectation value of the Γ_1-symmetry ground state in Si:P is plotted as a function of variational parameter b with (solid line) and without (dashed line) the intervalley kinetic energy.

and Ge:As are plotted in Figs. 6 and 7 against the radial distance r' (defined in ellipsoidal coordinates). The ground-state wave function calculated within the effective-mass approximation (EMA) is also included. It should be noted that the Γ_1-symmetry ground state is much more localized in space (therefore, more spread out in k space) than the other states. This is expected, because the tunneling of the wave function from a given valley to the other valleys has a large constructive effect for the Γ_1 state but small destructive effects for the Γ_3 and Γ_5 states. Therefore, the Γ_1 state should be more spread out in k space and more strongly bound, while the Γ_3 and Γ_5 states should be a bit less spread out in k space and less bound than the ground state of the single-valley Hamiltonian. However, as shown in Fig. 6, the ground state of Si calculated within EMA is more spread out than the Γ_3 and Γ_5 states. This is due to the neglect of the wave-vector dependence of the dielectric function that reduces the binding. The $l \neq 0$ components of the ground states are found to be negligibly small. The charge densities for the s-like components and d-like components of the Γ_1-symmetry excited states are plotted in Fig. 8 for Si:P and Fig. 9 for Ge:As, against the radial distance r'. From the nodal structure of the excited states shown in Figs. 8 and 9, it is noticed that the roles played by $3d_0$ and $4s$ states in Ge seem to be exchanged, as compared to that in Si. The charge distribution of all

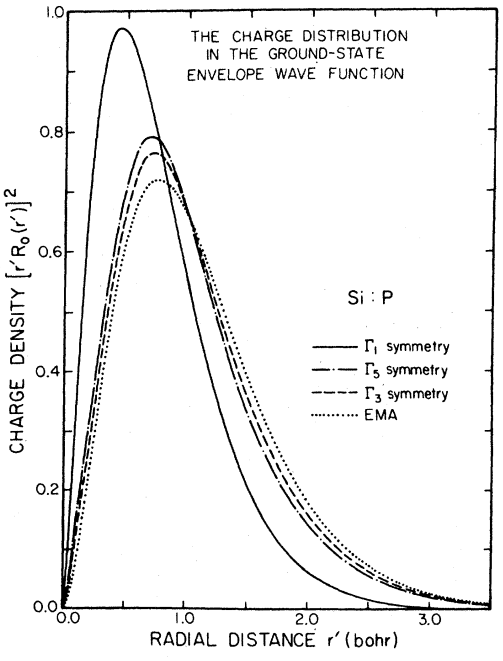

FIG. 6. Charge distribution in the ground-state envelope wave function for Si:P plotted against the radial distance r' (in ellipsoidal coordinate system) for various irreducible representations. The results obtained within EMA are also included for comparison.

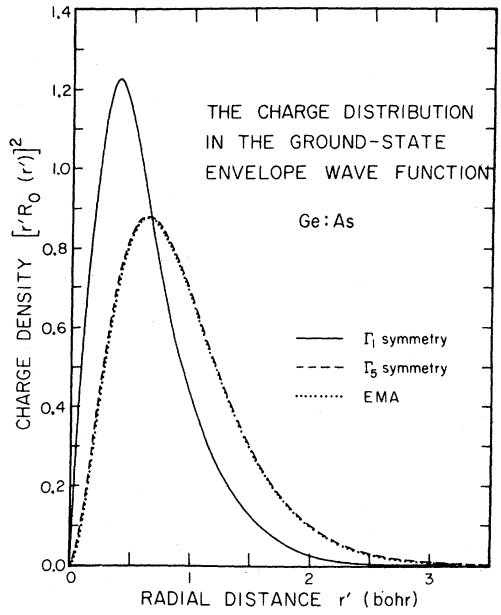

FIG. 7. Charge distribution in the ground-state envelope wave function for Ge:As plotted against the radial distance r' (in an ellipsoidal coordinate system) for various irreducible representations. The results obtained within EMA are also included for comparison.

the Γ_1-symmetry excited states except the $3d_0$ state in Si and the $4s$ state in Ge are found to be shifted toward the center with respect to the states obtained in EMA. This is expected, because the requirement of the orthogonality to the ground state (mainly s like) has substantially modified all the s-like excited-state wave functions. The $4s$ state in Ge, however, is intrinsically a $3d_0$ state as already mentioned and is not affected by the above requirement. On the other hand, the $3d_0$ state in Ge and $4d_0$ state in both Si and Ge, having the $4s$ and $5s$ nodal structures, are shifted toward the center to a small extent.

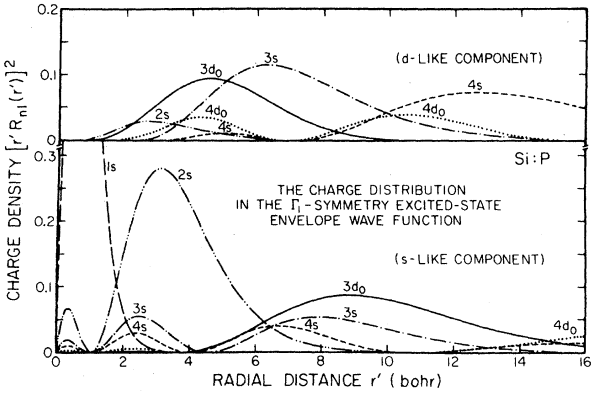

FIG. 8. Charge distribution in the Γ_1-symmetry excited-state envelope wave function for Si:P plotted against the radial distance r'.

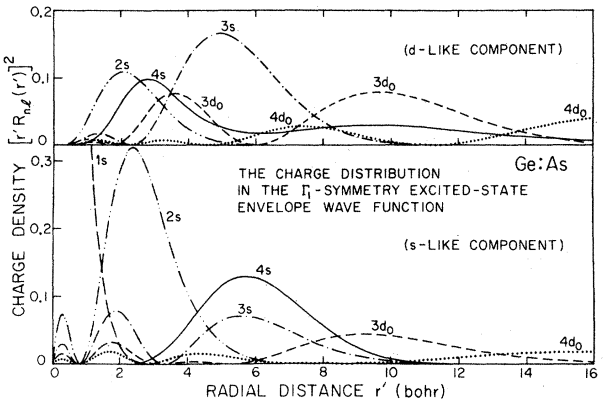

FIG. 9. Charge distribution in the Γ_1-symmetry excited-state envelope wave function for Ge:As plotted against the radial distance r'.

TABLE III. Short-range core potential strength parameters J_λ determined from fitting the calculated ground-state energies with the experimental data for nonisocoric impurities in Si and Ge. The units of J_λ are 10^{-3} Ry bohr^3.

Parameter \ Material	Si:As	Si:Sb	Si:Li	Ge:P	Ge:Sb
J_1	18.62	36.83	57.36	0.975	8.05
J_2	−4.88	−3.92	83.43	0.975	8.05
J_3	2.62	26.33	90.88	. . .	. . .

TABLE IV. Ionization energies of the six lowest $s(d)$-like states for various impurities in Si and Ge. The available experimental values are included in parentheses. All energy values are in meV.

			$1s$	$2s$	$3s$	$3d_0$	$4s$	$4d_0$
Si	Γ_1	P	45.5 (45.5)[a]	10.3 (10.6)[b]	5.22 (5.3)[b]	3.75 (3.75)[c]	3.11 (3.1)[b]	2.16 (2.2)[b]
		As	53.7 (53.7)[b]	10.9 (11.2)[b]	5.39 (5.3)[b]	3.75	3.20 (3.2)[b]	2.19 (2.2)[b]
		Sb	42.7 (42.7)[a]	10.0	5.15	3.75	3.07	2.14
		Li	31.2 (31.2)[d]	8.85	4.76	3.74	2.86	2.10
	Γ_5	P	34.2 (33.9)[a]	9.19 (9.05)[c]	4.88	3.75	2.92	2.11
		As	32.6 (32.6)[a]	9.01	4.82	3.75	2.89	2.10
		Sb	32.9 (32.9)[a]	9.04	4.83	3.75	2.89	2.10
		Li	33.0 (33.0)[b]	9.06 (9.0)[b]	4.84 (4.8)[b]	3.75	2.90	2.10
	Γ_3	P	32.7 (32.6)[a]	9.03 (9.05)[c]	4.82	3.75	2.89	2.10
		As	31.2 (31.2)[a]	8.85	4.76	3.75	2.86	2.10
		Sb	30.5 (30.5)[a]	8.76	4.73	3.74	2.84	2.10
		Li	33.0 (33.0)[b]	9.06 (9.0)[b]	4.84 (4.8)[b]	3.75	2.90	2.10
Ge	Γ_1	P	12.9 (12.9)[e]	3.90	2.27	1.51	1.20	0.96
		As	14.2 (14.2)[e]	4.01 (4.1)[f]	2.32 (2.4)[f]	1.53 (1.5)[f]	1.20	0.97
		Sb	10.3 (10.3)[e]	3.65	2.16	1.45	1.19	0.94
	Γ_5	P,As,Sb	9.81	3.59	2.14	1.43	1.19	0.94
		P	(10.1)[e]					
		As	(10.0)[e]					
		Sb	(10.0)[e]					

[a]Reference 30.
[b]Reference 31.
[c]Reference 32.
[d]Reference 33.
[e]Reference 34.
[f]Reference 35.

For nonisocoric impurities, we can adjust the core potential strength J_λ such that the calculated ground-state energies fit the experimental data, with the umklapp renormalization factors R_λ determined from the results for the isocoric impurities. In Table III, we listed the parameters J_λ determined for various impurities in Si and Ge. For the interstitial impurity Li in Si, we have used the umklapp renormalization factors, $R_2=1.08$ and $R_3=1.23$ (from Ref. 13). It should be noted that for zero core potential ($J_\lambda=0$), we obtain a large binding energy (about 600 meV) for the interstitial donors in Si. The energy eigenvalues for the states for various impurities in Si and Ge are listed in Table IV. The available experimental data[30–35] are also included in parentheses for comparison. Excellent agreement between theory and experiment is obtained. In Table IV, it is noticed that the ionization energies of the $3d_0$ state in Si and the $4s$ state (having the $3d_0$ nodal structure) in Ge are almost independent of impurity type and the valley-orbit interaction while the ionization energies of the other states are more or less affected. This is again due to the fact that the s-like excited states have to be readjusted to become orthogonalized to the new ground state, which has been modified by the valley-orbit interaction.

V. SUMMARY

We have constructed the model Hamiltonian for the donors in Si and Ge. The matrix elements of this model Hamiltonian can be expressed analytically, if Slater-type basis wave functions are used. This Hamiltonian yields almost identical results as the exact Hamiltonian, and because of its simplicity, can be applied to more complicated systems such as donor bound excitons and bound multiexciton complexes. We have also calculated the six lowest-energy eigenvalues for the $s(d)$-like states of each symmetry for various impurities in Si and Ge. Our results are in excellent agreement with the available experimental data.

ACKNOWLEDGMENTS

The authors gratefully acknowledge K. R. Elliott for useful technical discussions. The authors would like to thank M. Altarelli and W. Y. Hsu for providing them the Bloch functions $\phi_{k_j}^0$ at the band minima in Si used for the evaluation of J_λ's for Si:P. This work was supported in part by the Office of Naval Research under Contract No. N00014-75-C-0423.

APPENDIX A: FUNCTIONAL FORM FOR THE MODEL POTENTIALS

In the spherical model, the intervalley potentials are equal to their spherical average, i.e.,

$$V^{(\lambda)}(\vec{r})=J_\lambda\delta(\vec{r})-R_\lambda e^2\int e^{i(\vec{k}_j-\vec{k}_i)\cdot\vec{r}}\frac{1}{\epsilon(r)r}\frac{d\Omega}{4\pi}=J_\lambda\delta(\vec{r})-R_\lambda\frac{e^2}{\epsilon(r)r}\frac{\sin(\Delta_\lambda r)}{(\Delta_\lambda r)}\ , \tag{A1}$$

where $\Delta_\lambda\equiv|\vec{k}_i-\vec{k}_j|$ for $\lambda=1,2,3$ as before. In an ellipsoidal coordinate system [with $\vec{r}'\equiv(x,y,z/\zeta)$], the spherical average for $V^{(\lambda)}(\vec{r})$ is

$$V_S^{(\lambda)}(\vec{r}')=J_\lambda\int\delta(\vec{r})\frac{d\Omega'}{4\pi}-R_\lambda e^2\int e^{i(\vec{k}_j-\vec{k}_i)\cdot\vec{r}}\frac{1}{\epsilon(r)r}\frac{d\Omega'}{4\pi}\ . \tag{A2}$$

Comparing Eq. (A2) with Eq. (A1), we can approximate $V_S^{(\lambda)}(\vec{r})$ by the expression

$$V_{SM}^{(\lambda)}(\vec{r}')=J_\lambda\frac{\delta(\vec{r}')}{\zeta}-R_\lambda\frac{e^2}{\epsilon'(r')r'}\frac{f_\lambda a_0\sin(p_\lambda\Delta r')}{(p_\lambda\Delta r')}\ , \tag{A3}$$

where

$$\frac{1}{\epsilon'(r')}\equiv\frac{1}{\epsilon_0}\sum_{\nu=1}^{4}S_\nu e^{-h\sigma_\nu r'}\ ,\quad \Delta\equiv2\zeta k_0\ ,\quad a_0\equiv\int_0^1\frac{d(\cos\theta')}{(1-g^2\cos\theta')^{1/2}}=\frac{\sin^{-1}g}{g}\ ,$$

with $g^2\equiv1-\zeta^2$ and f_λ, p_λ, and h are adjustable parameters.

APPENDIX B: MATRIX ELEMENTS FOR INTERVALLEY KINETIC ENERGY

In this appendix we derive a simplified expression for Eq. (36) for the intervalley KE matrix elements. Substituting Eq. (22) and Eq. (35) into Eq. (36), we obtain

$$\langle b_2|T^{(2)}|b_1\rangle = \frac{\zeta(b_1b_2)^{5/2}}{4\pi}\int_0^\infty k_\zeta dk_\zeta \int_{-\beta/2}^{\pi-\beta/2} d\phi \int_{-\infty}^{\infty} dk_x \times \frac{(1/\mu)(k_z-k_0)^2+k_x^2+k_y^2}{[b_2^2+k_x^2+\zeta^2(k_t-k_0)^2+k_s^2]^2[b_1^2+k_x^2+k_y^2+\zeta^2(k_z-k_0)^2]^2}+\cdots , \tag{B1}$$

where the ellipses here and following represent exchange terms, and with $k_t \equiv k_\zeta\cos(\phi+\beta)$ and $k_s \equiv k_\zeta\sin(\phi+\beta)$ and

$$\langle b_2|T^{(3)}|b_1\rangle = (b_1b_2)^{5/2}\int_0^\infty dk_z\int_{-\infty}^{\infty}dk_x\int_{-\infty}^{\infty}dk_y \times \frac{(1/\mu)(k_z-k_0)^2+k_x^2+k_y^2}{[b_2^2+k_x^2+k_y^2+\zeta^2(k_z+k_0)^2]^2[b_1^2+k_x^2+k_y^2+\zeta^2(k_z-k_0)^2]^2}+\cdots , \tag{B2}$$

where we have used $k_\zeta\cos\phi = k_z$ and $k_\zeta\sin\phi = k_y$ and extended the region of integration to infinity along the direction where the function in the integral quickly decreases to zero as k increases. For $\lambda=2$, only the integration over k_x can be carried out analytically (we have chosen the x axis normal to the plane spanned by the two valleys).

$$\langle b_2|T^{(2)}|b_1\rangle \simeq \frac{\zeta(b_1b_2)^{5/2}}{2}\int_0^\infty dk_\zeta k_\zeta\int_{-\beta/2}^{\pi-\beta/2}d\phi\frac{I(k_\zeta,\phi)[(1/\mu)(k_z-k_0)^2+k_y^2]+1}{pq(p+q)^3}+\cdots , \tag{B3}$$

where

$$I(k_\zeta,\phi)=\left[\frac{1}{p^2}+\frac{1}{p^2}+\frac{3}{pq}\right] ,$$

$$p^2 \equiv b_1^2+\zeta^2(k_\zeta\cos\phi-k_0)^2+k_\zeta^2\sin^2\phi ,$$

$$q^2 \equiv b_2^2+\zeta^2[k_\zeta\cos(\phi+\beta)-k_0]^2+k_\zeta^2\sin^2(\phi+\beta) ,$$

where $\beta=90°$ for Si and 109.47° for Ge. For $\lambda=3$, only the integration over k_x and k_y can be carried out analytically.

$$\langle b_1|T^{(3)}|b_2\rangle = \frac{2\zeta(b_1b_2)^{5/2}}{\pi^2}\int_0^\infty dk_z[(1/\mu)(k_z-k_0)^2I(k_z)+J(k_z)]+\cdots , \tag{B4}$$

where

$$I(k_z)=\frac{1}{(p_+-p_-)^2}\left[\frac{1}{p_+}+\frac{1}{p_-}\right]-\frac{2}{(p_+-p_-)^3}\ln\left[\frac{p_+}{p_-}\right]$$

and

$$J(k_z)=\frac{(p_++p_-)}{(p_+-p_-)^3}\ln\left[\frac{p_+}{p_-}\right]-\frac{2}{(p_+-p_-)^2} ,$$

with

$$p_+ \equiv b_1^2+(k_z+k_0)^2\zeta^2 , \quad p_- \equiv b_2^2+(k_z-k_0)^2\zeta^2 .$$

The remaining integrals must be carried out numerically.

[1]J. M. Luttinger and W. Kohn, Phys. Rev. 97, 869 (1955).
[2]W. Kohn and J. M. Luttinger, Phys. Rev. 98, 915 (1955).
[3]R. A. Faulkner, Phys. Rev. 184, 713 (1969).
[4]B. A. Baldereschi, Phys. Rev. B 1, 4673 (1970).
[5]H. Fritzsche, Phys. Rev. 125, 1560 (1962).
[6]T. H. Ning and C. T. Sah, Phys. Rev. B 4, 3468 (1971).
[7]D. Schechter, Phys. Rev. B 8, 652 (1973).
[8]S. T. Pantelides and C. T. Sah, Phys. Rev. B 10, 621 (1974).

[9]S. T. Pantelides and C. T. Sah, Phys. Rev. B 10, 638 (1974).
[10]A. Sarker, J. Phys. C 10, 2617 (1977).
[11]K. Shindo and H. Nara, J. Phys. Soc. Jpn. 40, 1640 (1976).
[12]R. Resta, J. Phys. C 10, L179 (1977).
[13]M. Altarelli, W. Y. Hsu, and R. A. Sabatini, J. Phys. C 10, L605 (1977).
[14]D. C. Herbert and J. Inkson, J. Phys. C 10, L695 (1977).
[15]L. Resca and R. Resta, Solid State Commun. 29, 275 (1979).
[16]L. Resca and R. Resta, Phys. Rev. Lett. 44, 1340 (1980).
[17]J. R. Chelikowsky and M. L. Cohen, Phys. Rev. B 14, 556 (1976).
[18]S. T. Pantelides, Solid State Commun. 30, 65 (1979).
[19]F. Bassani, G. Iadonisi, and B. Preziosi, Rep. Prog. Phys. 37, 1099 (1974).
[20]H. Nara and A. Morita, J. Phys. Soc. Jpn. 21, 1852 (1966).
[21]P. K. W. Vinsome and D. Richardson, J. Phys. C 4, 2650 (1971).
[22]J. Bernholc and S. T. Pantelides, Phys. Rev. B 15, 4935 (1977).
[23]E. B. Hale and T. G. Castner, Phys. Rev. B 1, 4763 (1970).
[24]See, for example, P. M. Morse and H. Feshbach, *Method of Theoretical Physics* (McGraw-Hill, New York, 1953).
[25]For the transverse valley ($\lambda=2$), $0^{(\lambda)}$ is a rotation span angle β about the x (or y) axis. For Si, $\beta=90°$; for Ge, $\beta=109.47°$. For the longitudinal valley ($\lambda=3$), $\beta=180°$ for Si. The $\lambda=3$ term is absent in Ge.
[26]See, for example, E. U. Condon and G. H. Shortley, *The Theory of Atomic Spectra* (Cambridge University Press, London, 1967), Chap. 6.
[27]Using these values, the expression (49) plus a point-charge potential represents the pseudopotential for Si:P obtained by Pantelides and Sah (Ref. 8) quite well.
[28]In this calculation, we have used the Bloch functions $\phi^0_{k_i}$ and $\phi^0_{k_j}$ obtained from Altarelli and Hsu (Refs. 13 and 29).
[29]M. Altarelli and W. Y. Hsu (private communication).
[30]R. L. Aggarwal and A. K. Ramdas, Phys. Rev. 140, A1246 (1965).
[31]R. Sauer, J. Lumin. 12/13, 495 (1976).
[32]M. L. W. Thewalt, Can. J. Phys. 55, 1463 (1977).
[33]R. L. Aggarwal, P. Fisher, V. Mourzine, and A. K. Ramdas, Phys. Rev. 138, A882 (1965).
[34]J. H. Reuszer and P. Fisher, Phys. Rev. 135, A1125 (1964).
[35]E. F. Gross, B. V. Novikov, and N. S. Soklov, Sov. Phys.—Solid State 14, 368 (1972) [Fiz. Tverd. Tela 14, 443 (1972)].